Nat Hazards (2015) 76:1911–1926
DOI 10.1007/s11069-014-1575-8

ORIGINAL PAPER

Landslide erosion associated with the Wenchuan earthquake in the Minjiang River watershed: Implication for landscape evolution of the Longmen Shan, eastern Tibetan Plateau

Feng Liu · Jianfeng Li · Shunhu Yang

Received: 17 July 2014 / Accepted: 23 December 2014 / Published online: 23 January 2015

Abstract In tectonically active mountain belts, earthquakes can contribute to surface erosion by generating large-scale landslides. This study focuses on establishing the relationship between surface erosion caused by the earthquake-induced landslides and landscape evolution of the Longmen Shan, eastern Tibet Plateau. The inventory of landslides related to the 2008 Wenchuan earthquake in the Minjiang River watershed was based on high-resolution remote sensing images and field surveys. The estimated landslide erosion rate related to the Wenchuan earthquake is of the order 0.4–0.6 mm $year^{-1}$ on both sides of the Minjiang River and its tributaries. This erosion is similar to erosion rates of 0.5–0.8 mm $year^{-1}$ measured by low-temperature thermochronology over a Myr-timescale. The landslides associated with repeated large earthquakes may contribute to this Myr-timescale surface erosion via enhanced erosion efficiency. Post-seismic high-resolution digital elevation models covering the period from 2008 and 2012 were compared to quantify fluvial erosion in the Baisha River, a tributary of the Minjiang River. The volume of eroded materials was approximately 1.9×10^4 m^3 over the 4-year period. In addition, the rapid removal of co-seismic knickpoints indicates significant post-seismic river transportation. If large earthquakes, such as the Wenchuan earthquake, have occurred at intervals of 2,000–3,000 years, then the associated rapid landslide erosion together with fluvial erosion during inter-seismic intervals may have played an important role in shaping the present landscape of the Longmen Shan.

Keywords Wenchuan earthquake · Landslide · Surface erosion · Landscape evolution · Minjiang River · Longmen Shan

F. Liu (✉) · J. Li
Institute of Geomechanics, Chinese Academy of Geological Sciences, Beijing 100081, China
e-mail: casinsar@gmail.com

S. Yang
Institute of Geology and Geophysics, Chinese Academy of Sciences, Beijing 100029, China

1 Introduction

The Ms 8.0 Wenchuan earthquake of May 12, 2008, which occurred in the Longmen Shan thrust fault zone, was the greatest intra-continental earthquake in China (Fu et al. 2008, 2011; Zhang et al. 2008; Xu et al. 2009a) (Fig. 1). The Wenchuan earthquake induced widespread landslides along valleys, as well as producing surface ruptures (Qi et al. 2010; Fu et al. 2011; Dai et al. 2011; Gorum et al. 2011). The Wenchuan Earthquake Fault Scientific Drilling Project (WFSD), initiated following the earthquake, reported a zone of fault gouge with a maximum thickness of 3.79 m along the Yingxiu–Beichuan fault zone. This thick section of fault gouge indicates long-term repeated seismic activity in the Longmen Shan thrust belt (Li et al. 2013). Earthquakes and associated landslides play a significant role in mountain building and landscape evolution in tectonically active mountain belts (Keefer 1994; Hovius et al. 1997, 2000, 2011; Dadson et al. 2004; Malamud et al. 2004; Avouac 2008; Ouimet 2011). In the Longmen Shan, previous studies focused on the volume balance between co-seismic rock uplift and eroded material generated by co-seismic landslides to determine whether large dip- and oblique-slip earthquakes have contributed to the high mountains (Parker et al. 2011; Li et al. 2014a, b; Ren et al. 2014a). However, few studies have focused on the combined role of repeated large earthquakes and fluvial erosion shaping the present topography in the Longmen Shan.

In this article, we focus on the Minjiang River watershed, which is characterized by high relief and experienced extensive earthquake-induced landslides in 2008. Based on interpretations of the post-earthquake high-resolution remote sensing images and field surveys, an inventory of earthquake-induced landslides on both sides of the Minjiang River and its tributaries has been developed. We quantify the erosion rate due to earthquake-induced landslides and compare this with erosion rates on Myr-timescale to evaluate the

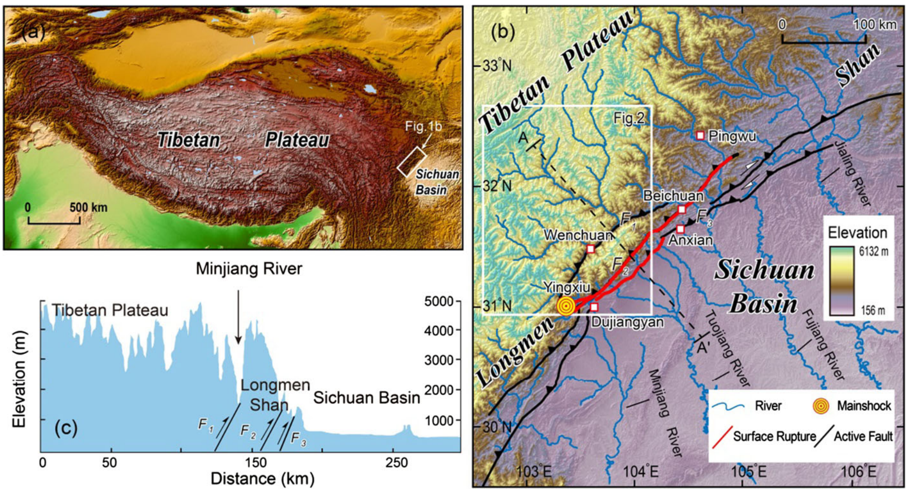

Fig. 1 **a** The Longmen Shan is located at the boundary between the Sichuan Basin and the eastern margin of the Tibetan Plateau. **b** Topography and active faults (F_1–F_3) in the Longmen Shan. F_1, Wenchuan–Maoxian fault; F_2, Yingxiu–Beichuan fault; F_3, Guanxian–Anxian fault; *Red lines* indicate the surface rupture associated with the Wenchuan earthquake. **c** A cross-sectional profile of the topography along AA′ (*dashed line*) is shown

role of the earthquake-induced landslides in surface processes. Furthermore, we discuss the implications of landslide erosion related to repeated larger earthquakes and fluvial erosion on the landscape evolution of the Longmen Shan.

2 Study area

The Longmen Shan resides in a region of steep topography in southeastern China and is the boundary between the Tibetan Plateau and Sichuan Basin (Fig. 1a). The Longmen Shan thrust fault zone is approximately 500 km long and 30–50 km wide and consists of three main sub-parallel faults (Deng et al. 1994; Burchfiel et al. 1995) that experienced thrust and dextral deformation along the major fault systems (Burchfiel et al. 1995; 2008; Kirby et al. 2002). From northwest to southeast, the three main faults are the Wenchuan–Maoxian fault (F_1), Yingxiu–Beichuan fault (F_2), the primary structure responsible for the 2008 Wenchuan earthquake (Zhang et al. 2008; Xu et al. 2009a), and Guanxian–Anxian fault (F_3) (Fig. 1b). The Wenchuan earthquake produced a surface rupture over 300 km long (Fu et al. 2008; Zhang et al. 2008; Xu et al. 2009a). The surface deformation was characterized by oblique thrust/dextral slip with a maximum vertical displacement of 9–10 m (Fu et al. 2008, 2011; Li et al. 2008; Ran et al. 2010a; Xu et al. 2009a; Zhang et al. 2010a). The Wenchuan earthquake induced massive landslides that are linearly distributed along the surface rupture zones and river valleys (Huang and Li 2009; Qi et al. 2010; Dai et al. 2011; Fu et al. 2011). In total, the earthquake triggered more than 56,000 landslides (Dai et al. 2011; Gorum et al. 2011; Xu et al. 2014). The main types of landslides were shallow landslides, rock falls, deep-seated landslides, and rock avalanches (Qi et al. 2010; Dai et al. 2011) that ranged in size from a few cubic meters to tens of millions of cubic meters (Dai et al. 2011). The estimated volume of the vast Daguangbao landslide located in Anxian county, the largest of the co-seismic landslides, is at least 7.4 km^3 (Huang et al. 2008; Yin et al. 2011; Chen et al. 2014).

The surface in the Longmen Shan has been deeply dissected by several major rivers (e.g., the Minjiang River, Tuojiang River and Fujiang River) (Fig. 1b). The landforms are characterized by steep hillslopes and deep-incised valleys (Fig. 1c). Originating in the eastern margin of the Tibetan Plateau, the Minjiang River flows along the Wenchuan–Maoxian fault (F_1), passes through the Longmen Shan Range cutting gorges more than 1–3 km deep (Burchfiel et al. 1995), and drains into the Sichuan Basin at Dujiangyan. The study area presented here is confined to the Minjiang drainage basin within the Longmen Shan Range (Fig. 2a). The Baisha River is a tributary of the Minjiang River (Fig. 2a). The Wenchuan earthquake produced a surface rupture over 14 km long along this river (Fig. 2b) (He et al. 2008a). A co-seismic knickpoint with a height of about 4.5 m was formed in the Baisha River at Bajiaomiao village near the town of Hongkou (Liu-Zeng et al. 2010).

The eastern margin of the Tibetan Plateau is influenced by a wet tropical climate. Monsoon rainfall dominates with annual precipitation as high as 1,000 mm $year^{-1}$ in the Longmen Shan (Godard et al. 2010). Most of the precipitation is concentrated during the heavy rains of the summer monsoon from June through September, and this constitutes 70–80 % of the total annual rainfall. Thus, water discharge shows a strong monsoonal influence (Liu-Zeng et al. 2011) and sediment transport away from the Longmen Shan, with 80–90 % of the annual suspended sediment transport occurring from June to September (Liu-Zeng et al. 2011).

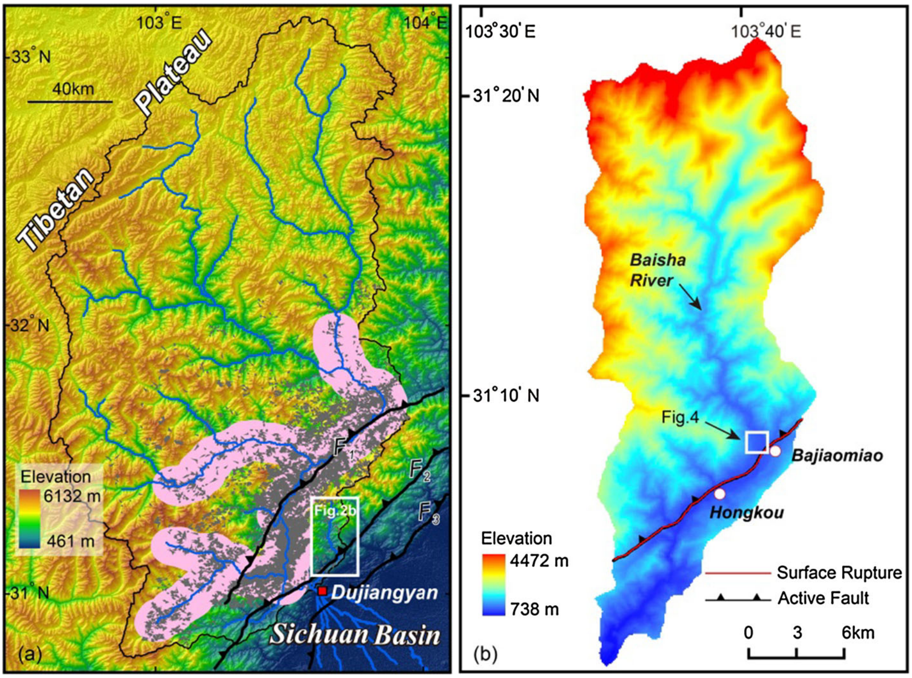

Fig. 2 **a** *Shaded relief map* shows the morphology of the Minjiang drainage basin. $F_{1,}$ Wenchuan–Maoxian fault; F_2, Yingxiu–Beichuan fault; F_3: Guanxian–Anxian fault. The landslides have a zonal distribution along the main channel of the Minjiang River and its tributaries. **b** A 14-km long surface rupture was produced by the Wenchuan earthquake along the Baisha River (He et al. 2008a)

3 Data and methodology

Owing to severe weather conditions, cloud- and haze-free images of the study region were difficult to obtain. Consequently, multi-source and multi-temporal remotely sensed images were collected after the Wenchuan earthquake with the aim of identifying earthquake-induced landslides. The landslide inventory was based on interpretations of aerial photographs (with 1-m spatial resolution) obtained on May 16–24, 2008, SPOT images (with 10-m spatial resolution) obtained on May 23, 2008, and Aster images (with 15-m spatial resolution) obtained on May 14–15, 2008. All images were processed and analyzed using image analysis and GIS software, such as ENVI 4.8 and ArcGIS 9.3. The images were geo-referenced using ground control points (GCPS) selected from 1:50,000 scale digital topographic maps. The root mean square error (RMSE) of the accuracy of the geo-referencing was set to not exceed the size of a pixel. All images were projected on a Universal Transverse Mercator (UTM) zone 48 North projection using the WGS84 datum.

3.1 Landslide detection

Landslides were identified on the basis of one or more diagnostic features including morphology, vegetation, and tones of the images (Yang and Chen 2010; Dai et al. 2011). Morphological characteristics included slope angle, visible landslide debris movement paths, and run-out lobe forms. The landslides were also recognized from newly denuded vegetation on the slope, linear scars in vegetation along run-out paths, and disturbed vegetation on body contrast with surroundings on the images. Color characteristics of individual landslides were enhanced using the presence of bright white or dark brown contrast as compared to the surroundings. Landslide perimeters were captured through heads-up digitizing in ArcGIS and included both deposit and source area. For a larger landslide, the source area and deposit should be separated. Based on the above criteria, all landslides visible on the images were delineated as single polygons in ArcGIS and the total number of landslides and the areas of individual landslide were calculated.

3.2 Earthquake-induced landslide erosion

Quantifying the erosion rate is a useful way of identifying the contribution of earthquake-induced landslides to surface erosion. In the Longmen Shan, long-term seismic activity occurs along the Yingxiu–Beichuan fault zone (Li et al. 2013). In addition, the recurrence interval of large earthquakes similar to the Wenchuan earthquake is in the range 2,300–3,300 year (Ran et al. 2010b, 2013; Chen et al. 2013). We assumed that a large earthquake similar to the Wenchuan earthquake is the characteristic earthquake within the Longmen Shan region.

For a characteristic earthquake, the earthquake-induced landslide erosion rate can be measured by the following equation (Malamud et al. 2004),

$$E_L = V_{TL}/A_L \times T_L \tag{1}$$

where E_L is the earthquake-induced landslide erosion rate, V_{TL} is the total landslide volume, A_L refers to the area over which the landslides are concentrated, and T_L is the time interval over which the landslides accumulated. For the earthquake-induced landslide event inventory, T_L can also be defined as the recurrence interval of an earthquake (Malamud et al. 2004). The total volume (V_{TL}) of earthquake-induced landslides is defined as follows,

$$V_{TL} = \sum_{i=1}^{N} V_{LN} \tag{2}$$

where N is the total number of landslides and V_{LN} is volume of an individual landslide. Each individual volume can be estimated from the empirical relationship between landslide volume and area (Simonett 1967; Rice et al. 1969; Hovius et al. 1997; Korup 2005; Imaizumi et al. 2008; Guzzetti et al. 2009; Parker et al. 2011; Li et al. 2014b).

Parker et al. (2011) and Li et al. (2014b) provided the formulas to estimate the landslide volume associated with the Wenchuan earthquake. However, due to the various kinds of co-seismic landslides present (Qi et al. 2010; Dai et al. 2011) and the ruggedness and inaccessibility of the terrain, it was difficult to obtain enough representative field data to establish the empirical relationship between the co-seismic landslide volume and area within the Longmen Shan. In contrast, Guzzetti et al. (2009) proposed a robust global scaling law, in which the relationship between landslide volume (V) and area (A) is largely independent of the physiographical setting. The formula of Guzzetti et al. (2009) to estimate each individual landslide volume is as follows:

$$V = 0.074 \times A^{1.450} \tag{3}$$

To test whether Guzzetti et al.'s (2009) equation could be applied to the landslides associated with the Wenchuan earthquake, four co-seismic landslides reported by Xu et al. (2009b) were selected to validate the equation (Table 1). Figure 3 shows that the trend of

Table 1 The area and volume of landslides associated with the Wenchuan earthquake (data from Xu et al. 2009b)

Name	Longitude (°)	Latitude (°)	Area (m^2)	Volume (m^3)
Laoyingyan	104.145	31.623	3.2×10^5	1.5×10^7
Donghekou	105.115	32.405	1.08×10^6	1.5×10^7
Woqian	104.966	32.309	7.0×10^5	1.2×10^7
Pingxi village	104.943	32.276	3.7×10^4	6.5×10^5

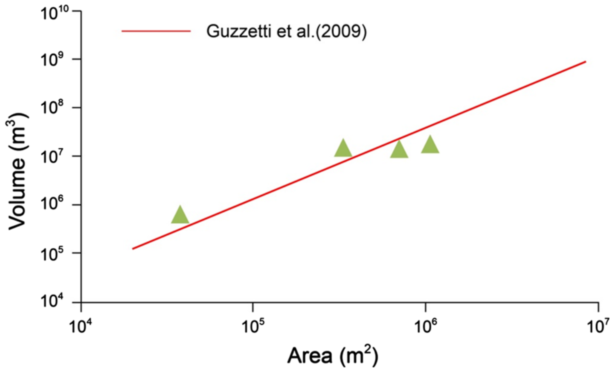

Fig. 3 Area–volume relationship (Guzzetti et al. 2009) with Wenchuan earthquake-induced landslides superimposed

Xu et al.'s (2009a, b) data is consistent with the power-law relationship of Guzzetti et al.'s (2009). In addition, the main Quaternary (*Q*) strata in the Longmen Shan are near horizontal or with a gentle slope and are therefore not generally prone to slide. Massive landslides mainly occurred in pre-Tertiary (*T*) strata, accounting for more than 92 % of the total landslides (Qi et al. 2010). The above-mentioned correlation between landslides and lithology shows that most landslides associated with the Wenchuan earthquake can be thought to be rock landslides. For bedrock landslides, Larsen et al. (2010) suggested that landslide erosion was controlled by hillslope material, and the relationship of individual landslide volume (V) and area (A) takes the form of a power law: $V = \alpha A^{\gamma}$ (α, γ are constant) with a scaling exponent $\gamma = 1.3$–1.6. The exponent 1.45 of Guzzetti et al.'s (2009) falls in the range 1.3–1.6. Thus, the Eq. (3) can be used to estimate individual landslide volume in the Longmen Shan.

Based on the method of Malamud et al. (2004), the area of the landslides concentration (A_L) is a rough estimate according to its spatial distribution in which a high percentage of landslides are concentrated. Note that the area is not necessarily as large as the area over which the landslide inventory was originally compiled. Furthermore, we defined the area of the landslide concentration (A_L) and assumed that erosion in this area is dominated by these landslides. The area A_L has a zonal distribution in the Minjiang River watershed. According to the spatial distribution (Huang and Li 2009; Qi et al. 2010; Dai et al. 2011), the area of the landslides concentrated (A_L) was calculated based on the extent of the Minjiang River and its tributaries within which an overwhelming majority of landslides were located.

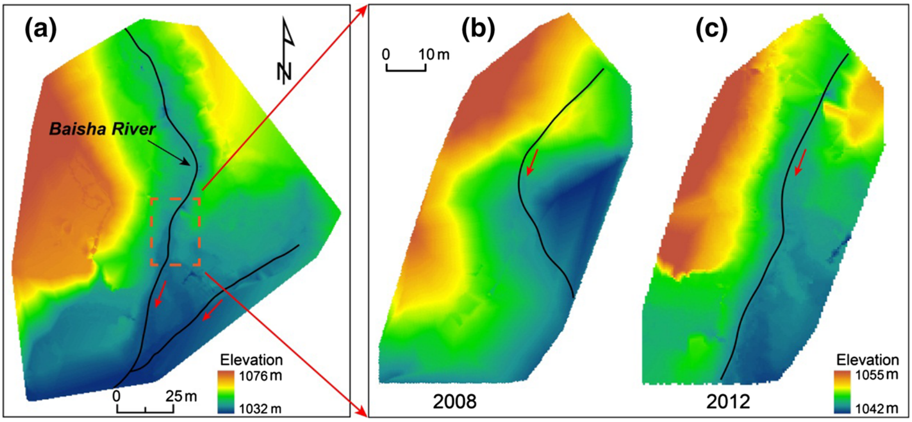

Fig. 4 Post-seismic fluvial erosion of the Baisha River in the 4 years following the Wenchuan earthquake. **a** DEM of the Bajiaomiao reach. **b** DEM produced from Total Station data collected in 2008. **c** DEM produced from Real-Time-Kinematic Global Positioning System data collected in 2012

3.3 Determining post-seismic river erosion

To elucidate the river erosion after the Wechuan earthquake, we used the Baisha River as a case study. The river erosion after the Wenchuan earthquake was estimated based on a comparison between 2008 and 2012 digital elevation models (DEM) compiled from the field measurement. Surveys were carried out using a Topokon total station (TS) and real-time-kinematic global positioning system (RTK-GPS) in 2008 and 2012, respectively. To minimize error and uncertainty, areas that were relatively undisturbed by human activity were selected for analysis. Kriging was used to interpolate via ArcGIS to obtain the final DEM with a spatial resolution of 0.5 m. Finally, all DEMs were geo-referenced to the coordinate system WGS84 UTM.

4 Results

4.1 Earthquake-induced landslide erosion

Based on aerial photographs and satellite images, 7,567 landslides were identified along the main channel of the Minjiang River within 8,000 m of the drainage line (Fig. 2a). Based on this distance, the area of landslide concentration (A_L) was measured as 4,520 km^2 with the aid of ArcGIS. Combining Eqs. (2) and (3), the total volume (V_{TL}) of the 7,567 landslides was estimated to be about 5.7–5.9 km^3.

Historical records indicate no earthquakes larger than magnitude 7 have been reported in the Longmen Shan region (Wen et al. 2009). Pre-earthquake trenches along the Yingxiu–Beichuan fault zone show an earthquake recurrence interval of at least 2,000–3,000 years (Li et al. 2006). Post-earthquake trench excavation indicates that the recurrence interval of large earthquakes similar to the Wenchuan earthquake is in the range 2,300–3,300 year (Ran et al. 2010b, 2013; Chen et al. 2013). From these studies, it may be concluded that large earthquakes have a recurrence interval of 2,000–3,000 years. For the characteristic earthquake, the repeated time of co-seismic landslides is the recurrence interval of the earthquake (Malamud et al. 2004). Thus, the time interval over which co-seismic landslides accumulated is 2,000–3,000 years. From Eq. (1), the average erosion rate (E_L) due to earthquake-induced landslides is estimated to be 0.4–0.6 mm year^{-1}. Our result falls in the range 0.1–0.6 mm year^{-1} reported by Parker et al. (2011).

4.2 Post-seismic river erosion

A comparison between the 2008 and 2012 DEMs from the Baisha River (Fig. 4) suggests that the river has removed at least volume of 1.9×10^4 m^3 of material during the 4 years after the 2008 Wenchuan earthquake. The surface ruptures of the Wenchuan earthquake caused the formation of the fluvial knickpoints (Fu et al. 2009; He et al. 2008a; Liu-Zeng et al. 2009; Xu et al. 2008). The knickpoints were rapidly removed during the post-earthquake period. For example, at Pingtong town, Pingwu county, the surface rupture cut through the river bed and formed a knickpoint with a height of about 2.3 m on May 12, 2008 (Xu et al. 2008), but this had been removed by river erosion within 1 month (He et al.

Fig. 5 *Field photographs* showing evidence of rapid fluvial erosion. **a** Knickpoint with a height of 4.5 m produced by co-seismic deformation in Hongkou, Dujiangyan City (Liu-Zeng et al. 2010). **b** The co-seismic knickpoint dissipated in 2012

2008b). Another knickpoint, with a height of nearly 4.5 m, was produced in the Baisha River by coseismic deformation (Liu-Zeng et al. 2010) (Fig. 5a). However, knickpoint was not present in 2012 (Fig. 5b).

5 Discussion

5.1 Assessing the uncertainties associated with estimating landslide volume

The present study of the 7,547 co-seismic landslides produced about 5.7–5.9 km^3 of hillslope material on both sides of the Minjiang River and its tributaries over an area of 4,500 km^2. In contrast, Parker et al. (2011) suggest that more than 50,000 landslides produced 5–15 km^3 of erodible material within the Longmen Shan region. The estimated landslide volume range of 5–15 km^3 was revised to 2.1–3.7 km^3, which is considered to be consistent with the range of 1.5–3.6 km^3 reported by Ren et al. (2014b). Compared with these results, we may have overestimated the landslide volume because we only determined the landslide volume of part of the area within the Longmen Shan.

Previous studies used various methods to reduce the uncertainties associated with the calculated landslide volumes related to the Wenchuan earthquake (Parker et al. 2011; Li et al. 2014b; Ren et al. 2014b). These studies used the robust scaling relationship between landslide volume and area (Parker et al. 2011; Li et al. 2014b), or topographic changes between pre- and post-earthquake DEMs (Ren et al. 2014b) to estimate the landslide volume. In contrast, we gave a rough estimate by an empirical formula, lacking a region calibration. However, an important problem must be addressed: How to quantify the effect of a gigantic landslide on the estimated total volume of all landslides? For example, the Daguangbao landslide is the largest co-seismic landslide within the Longmen Shan region (Huang et al. 2008; Yin et al. 2011). The volume of the Daguangbao landslide is 7.4–11.99 km^3 based on the differential DEM method (Huang et al. 2008; Yin et al. 2011). However, the volume of all co-seismic landslides is 2.1–3.7 km^3 (Li et al. 2014b). This discrepancy suggests that the estimated landslide volume may contain large uncertainties no matter which empirical relationship between landslide volume and area is used within the Longmen Shan. Nonetheless, the landslide erosion rate estimated here is of the same order of magnitude as that of Parker et al. (2011).

5.2 Earthquake-induced landslides and long-term surface erosion

Landslide erosion rates are needed for comparison with erosion rates derived from low-temperature thermochronology over a Myr-timescale to assess the importance of landslides in the landscape evolution of the Longmen Shan. Low-temperature thermochronology is an important tool for estimating rates of erosion in mountain landscapes (Safran 2003). Bedrock low-temperature thermochronology may provide erosion rates with a thermal model or by collecting multiple samples in a vertical transect via point measurements. Long-term erosion rates in the Longmen Shan obtained from low-temperature thermochronology are averaged over the past 10–15 Ma (Ouimet 2010). Low-temperature thermochronological data in the Minjiang River watershed are sparse and yield location-specific results. The average Myr-timescale erosion rates are 0.5–0.8 mm $year^{-1}$ in the Longmen Shan (e.g., Godard et al. 2009b). We assumed that this limited low-temperature thermochronological data can reflect the areal average erosion rate. The magnitude of the erosion rate due to earthquake-induced landslides (0.4–0.6 mm year^{-1}) is similar to the Myr-timescale erosion rates derived from low-temperature thermochronology.

Earthquakes are capable of triggering a large number of deep-seated bedrock landslides that are considered to be significant agents of rapid surface erosion (Hovius and Stark 2006). For example, landslide erosion rates increase significantly with increasing exhumation rate over the Myr-timescale in the eastern Himalaya syntaxis (Larsen and Montgomery 2012). In the Longmen Shan, the long-term erosion rates obtained from low-temperature thermochronology were averaged over the last 10 Ma (Kirby et al. 2002; Godard et al. 2009b). Therefore, during the Cenozoic topographic evolution of the Longmen Shan, the long-term (Myr-scale) erosion integrates many repeated earthquake events, which is confirmed by the result of the WSDF (Li et al. 2013). Large seismic events accelerate surface erosion by fracturing rock and mass wasting (Molnar et al. 2007). Fracturing can reduce rock strength, which leads to pervasive weathering of fractured rock along fracture planes and facilitates the extent of erosion. Mass wasting strips rock or soil from hillslope, thereby exposing fresh, unaltered rock to surface and making it easier to be eroded (Fig. 6). A recent study has shown that bare rock surfaces were eroded by 10–30 cm within 1 year of the Wenchuan earthquake (Wang et al. 2011). Thus, the massive landslides associated with repeated large earthquake and aftershocks may contribute to the long-term surface erosion by enhancing erosion efficiency.

5.3 Implications for the long-term landscape evolution of the Longmen Shan

The rapid removal of earthquake-generated knickpoints may indicate a significant fluvial erosion capacity during the post-earthquake period. Previous studies have shown that long-term storage of co-seismic sediment along the major Longmen Shan River valley is unlikely (Kirby et al. 2003; Ouimet et al. 2009), as it can be evacuated efficiently over the entire earthquake cycle (Parker et al. 2011). Similarly, Liu et al. (2013) reported that most of the landslide-eroded sediment due to the Wenchuan earthquake is likely to be efficiently evacuated out of the Longmen Shan in the Minjiang River watershed over a seismic cycle. Seasonal floods could explain this efficient sediment delivery. In the field, we observed that heavy rainfall increases runoff and further sediment flux during the summer. In addition, a large volume of coarse-grained sediment deposited on the Chengdu Plain during the late

Fig. 6 Mass wasting exposes soil or fresh, unaltered rock to erosion. Photograph (**a**) and (**b**) are from Fu et al. (2009) and Yang and Chen (2010), respectively

Cenozoic has been interpreted to be closely associated with the region climate cycles and repeated large earthquakes similar to the Wenchuan earthquake (Wang and Meng 2009), indicating that the fluvial systems of the Longmen Shan have a high transport capacity.

The Wenchuan earthquake induced large-scale landslides along surface ruptures and river valleys (Huang and Li 2009; Fu et al. 2011). This spatial distribution mirrors the

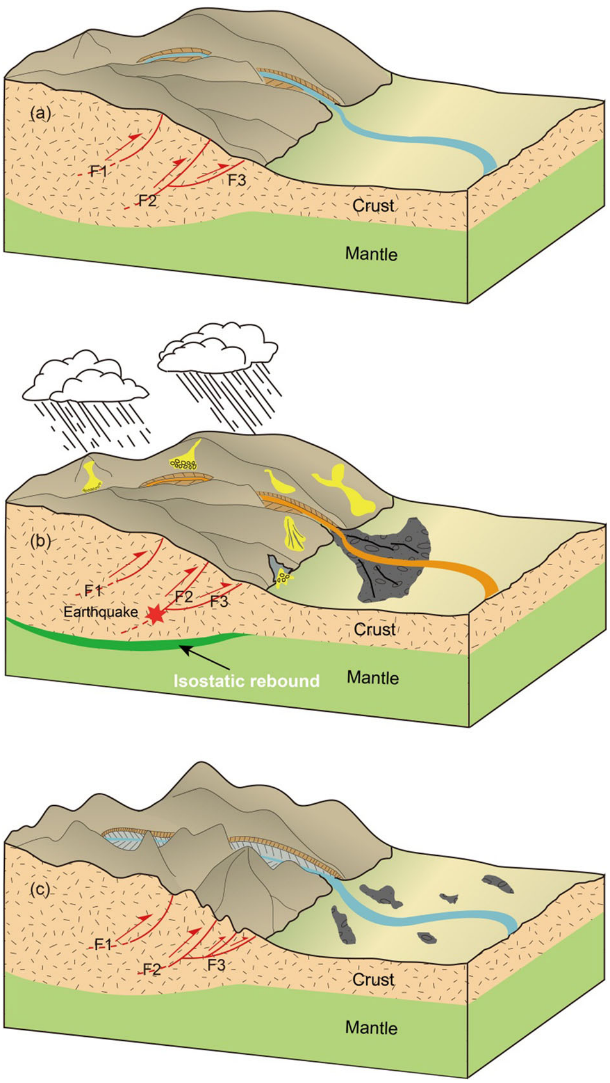

Fig. 7 Schematic model of landscape evolution in the Longmen Shan. **a** Mountain building with gentle slope produced by tectonic uplift. **b** Large earthquakes strike the Longmen Shan, exposing fresh rock and furthering the extent of surface erosion. Heavy rainfall results in rapid surface erosion. The material released by the mass wasting following large earthquake is transported out of the Longmen Shan by rivers, and this triggers isostatic rebound at the boundary between the lower crust and the upper mantle (*black arrow*) (Fu et al. 2011; Zhang et al. 2009, 2010b). **c** Erosional unloading results in preferential rock uplift focused along the major rivers. Tectonic uplift enhances river incision, which in turn creates the deep-incised valleys and high topographic relief

erosion, which is intense along rupture zones and river valleys. Similarly, the Myr-scale and modern denudation pattern show narrow zones of higher erosion rates along the active thrust fault (Godard et al. 2009a; Liu-Zeng et al. 2011). This relationship suggests that the earthquake-induced landslides may play a role in enhancing the differential erosion during the long-term landscape evolution. With the occurrence of repeated large earthquakes, long-term surface erosion produced by earthquake-triggered landslides, together with denudation related to other surface processes, may lead to unloading of the underlying lithosphere and consequent isostatic compensation, resulting in the uplift of summits of the Longmen Shan. This isostatic uplift is expected unless the erodible material is transported out of the Longmen Shan by rivers. In fact, the fluvial system has a significant capacity of transporting the erodible material out of the Longmen Shan. Thus, isostasy cannot be ignored in maintaining the high terrain of the Longmen Shan (Molnar 2012).

Late Cenozoic crustal shortening is a primary driver of uplift and the topographic development of the Longmen Shan (Hubbard and Shaw 2009; Tian et al. 2013). In this tectonic context, the fluvial system deeply incised the Longmen Shan, which produced the high relief. Without sustained endogenetic forces, the topography will be beveled by exogenic geological processes. The climate of the Longmen Shan and adjacent regions is characteristically warm and wet, with more precipitation in summer due to the influence of yearly monsoon. Several major rivers cross or originate from the Longmen Shan (Fig. 1). However, these rivers, and other surface erosion processes, do not degrade the topography. This leads to the question: How is the high relief of the Longmen Shan sustained? The long-term fluvial unloading related to the transport of eroded material due to earthquake-triggered landslides and other surface processes may induce isostatic rebound between the lower crust and upper mantle and result in deep mantle convection beneath the Longmen Shan (Fu et al. 2011; Liu et al. 2013). Consequently, deep tectonic processes may maintain the present-day steep topography of the Longmen Shan. Thus, rapid erosion associated with repeated large earthquakes and fluvial incision during the interseismic interval may be the important driver that is shaping the landscape of the Longmen Shan (Fig. 7).

6 Conclusions

Based on interpretations of high-resolution remote sensing images, 7,567 landslides were identified that were related to the Wenchuan earthquake within 8,000 m of the Minjiang River and its tributaries. The volume of erodible material was estimated to be 5.7–5.9 km^3. Assuming that estimated 2,000–3,000-year time interval over which the landslides accumulated is reasonable, the landslides on both sides of the Minjiang River produced an erosion rate of 0.4–0.6 mm $year^{-1}$. The earthquakes and associated erosion events may influence long-term (Myr-timescale) surface erosion by enhancing erosional efficiency. Furthermore, the rapid erosion associated with repeated large earthquakes similar to the Wenchuan earthquake, and river erosion during the interseismic interval, may contribute to the present-day landscape of the Longmen Shan area.

Acknowledgments This research was supported by the Project of the 12th Five-year National Sci-Tech Support Plan of China (2011BAK12B09), the Special Project of Basic Work of Science and Technology (2011FY110100-2), National Natural Science Foundation of China (41171009) and Geological Investigation Project of China Geological Survey (12120114002101, 1212011120099). We thank Daniel P. Miggins whose careful and thorough comments significantly improved this paper. Prof. Bihong Fu and Dr. Weiming Liu provided constructive comments that helped to strengthen the early version of this manuscript. This study benefited greatly from Total Station data provided by Prof. Haibing Li. We especially thank our colleagues Ming Liu and Genwen He for help in the field.

References

Avouac JP (2008) Dynamic processes in extensional and compressional settings-mountain building: from earthquakes to geological deformation. In: Watts AB (ed) Crustal and lithosphere dynamics (treatise on geophysics), vol 6. Elsevier, Amsterdam, pp 377–439

Burchfiel BC, Chen ZL, Lliu YP, Royden LH (1995) Tectonics of the Longmen Shan and adjacent region, central China. Int Geol Rev 37:661–735

Burchfiel BC, Royden LH, Vander Hilst RD, Hager BH, Chen ZL, King RW, Li C, Lü J, Yao H, Kirby E (2008) A geological and geophysical context for the Wenchuan earthquake of 12 May 2008, Sichuan, People's Republic of China. GSA Today 18:4–11

Chen LC, Ran YK, Wang H, Shi X, Liu RC, Dong SP (2013) Paleoseismology and kinematic characteristics of the Xiaoyudong rupture, a short but significant strange segment characterized by the May 12, 2008, Mw 7.9 earthquake in Sichuan, China. Tectonophysics 584:91–101

Chen Q, Cheng H, Yang Y, Liu G, Liu L (2014) Quantification of mass wasting volume associated with the giant landslide Daguangbao induced by the 2008 Wenchuan earthquake from persistent scatterer InSAR. Remote Sens Environ 152:125–135

Dadson SJ, Hovius N, Chen H, Dade WB, Lin JC, Hsu ML, Lin CW, Horng MJ, Chen TC, Milliman J (2004) Earthquake-triggered increase in sediment delivery from an active mountain belt. Geology 32:733–736

Dai FC, Xu C, Yao X, Xu L, Tu XB, Gong QM (2011) Spatial distribution of landslides triggered by the 2008 Ms 8.0 Wenchuan earthquake, China. J Asian Earth Sci 40:883–895

Deng QD, Chen SF, Zhao XL (1994) Tectonics, seismicity and dynamics of Longmen shan mountains and its adjacent regions. Seismol Geol 16:389–403 (in Chinese with English abstract)

Fu BH, Shi PL, Zhang ZW (2008) Spatial characteristics of the surface rupture produced by the Ms 8.0 Wenchuan earthquake using high-resolution remote sensing imagery. Acta Geol Sin 82:1679–1687 (in Chinese with English abstract)

Fu BH, Wang P, Kong P, Shi PL, Zheng GD (2009) Altas of seismological and geological disasters associated with the 12 May 2008 Ms 8.0 Wenchuan great earthquake, Sichuan, China. Seismological Press, Beijing, pp 97–99 (in Chinese and English)

Fu BH, Shi PL, Guo HD, Okuyama S, Ninomiya Y, Wright S (2011) Surface deformation related to the 2008 Wenchuan earthquake, and mountain building of the Longmen Shan, eastern Tibetan Plateau. J Asian Earth Sci 40:805–824

Godard V, Cattin R, Lavé J (2009a) Erosional control on the dynamics of low-convergence rate continental plateau margins. Geophys J Int 179:763–777

Godard V, Pik R, Lavé J, Cattin R, Tibari B, De Sigoyer J, Pubellier M, Zhu J (2009b) Late Cenozoic evolution of the central Longmen Shan, eastern Tibet: insight from (U–Th)/He thermo-chronometry. Tectonics 28:TC5009. doi:10.1029/2008TC002407

Godard V, Lavé J, Carcaillet J, Cattin R, Bourlès D, Zhu J (2010) Spatial distribution of denudation in Eastern Tibet and regressive erosion of plateau margins. Tectonophysics 491:253–274

Gorum T, Fan X, van Westen CJ, Huang RQ, Xu Q, Tang C, Wang G (2011) Distribution pattern of earthquake-induced landslides triggered by the 12 May 2008 Wenchuan earthquake. Geomorphology 133:152–167

Guzzetti F, Ardizzone F, Cardinali M, Rossi M, Valigi D (2009) Landslide volumes and landslide mobilization rates in Umbria, central Italy. Earth Planet Sci Lett 279:222–229

He HL, Sun ZM, Wei ZY, Dong SP, Gao X, Wang SY, Wang JQ (2008a) Rupture of the MS8.0 Wenchuan earthquake along Baishahe River. Seismol Geol 30:658–673 (in Chinese with English abstract)

He ZT, Ma BQ, Tian QJ, Zhang SM (2008b) Deformation features of surface rupture of the Wenchuan earthquake(M8.0) at the Pingtong town. Quat Sci 28:789–795 (in Chinese with English abstract)

Hovius N, Stark CP (2006) Landslide-driven erosion and topographic evolution of active mountain belts. In: Evans SG et al (eds) Landslides from massive rock slope failure. Springer, Berlin, pp 573–590

Hovius N, Stark CP, Allen PA (1997) Sediment flux from a mountain belt derived by landslide mapping. Geology 25:231–234

Hovius N, Stark CP, Chu HT, Lin JC (2000) Supply and removal of sediment in a landslide-dominated mountain belt: central Range, Taiwan. J Geol 108:73–89

Hovius N, Meunier P, Lin CW, Chen H, Chen YG, Dadson S, Horng MN, Lines M (2011) Prolonged seismically induced erosion and the mass balance of a large earthquake. Earth Planet Sci Lett 304:347–355
Huang RQ, Li WL (2009) Development and distribution of geohazards triggered by the 5.12 Wenchuan Earthquake in China. Sci China Ser E Technol Sci 52:810–819
Huang RQ, Pei XN, Li TB (2008) Basci characteristics and formation mechanism of the largest scale landslide at Daguangbao occurred during the Wenchuan earthquake. J Eng Geol 16:730–741 (in Chinese with English abstract)
Hubbard J, Shaw JH (2009) Uplift of the Longmen Shan and Tibetan plateau, and the 2008 Wenchuan (M = 7.9) earthquake. Nature 458:194–197
Imaizumi F, Sidle R, Kamei R (2008) Effects of forest harvesting on the occurrence of landslides and debris flows in steep terrain of central Japan. Earth Surf Proc Land 33:827–840
Keefer DK (1994) The importance of earthquake-induced landslides to long-term slope erosion and slope-failure hazards in seismically active regions. Geomorphology 10:265–284
Kirby E, Reiners PW, Krol MA, Whipple KX, Hodges KV, Farley KA, Tang WQ, Chen ZL (2002) Late Cenozoic evolution of the eastern margin of the Tibetan Plateau: inferences from 40Ar/39Ar and (U–Th)/He thermochronology. Tectonics 21(1001):2000. doi:10.1029/TC001246
Kirby E, Whipple KX, Tang WQ, Chen ZL (2003) Distribution of active rock uplift along the eastern margin of the Tibetan Plateau: inferences from bedrock channel longitudinal profiles. J Geophys Res 108:2217. doi:10.1029/2001jb000861
Korup Oliver (2005) Geomorphic hazard assessment of landslide dams in South Westland, New Zealand: fundamental problems and approaches. Geomorphology 66:167–188
Larsen IJ, Montgomery DR (2012) Landslide erosion coupled to tectonics and river incision. Nat Geosci 5:468–473
Larsen IJ, Montgomery DR, Korup O (2010) Landslide erosion controlled by hillslope material. Nat Geosci 3:247–251
Li Y, Zhou RJ, Densemore AL, Ellis MA (2006) Geodynamic processes of the eastern margin of the Tibetan plateau and its geological responses. Geological Publishing House, Beijing
Li HB, Fu XF, Van Der Woerd J, Si JL, Wang ZX, Hou LW, Qiu ZL, Li N, Wu FY, Xu ZQ, Tapponnier P (2008) Co-seismic surface rupture and dextral-slip oblique thrusting of the Ms 8.0 Wenchuan earthquake. Acta Geol Sin 82:1623–1643 (in Chinese with English abstract)
Li HB, Wang H, Xu ZQ, Si JL, Pei JL, Li TF, Huang Y, Song SR, Kuo LW, Sun ZM, Chevalier ML, Liu DL (2013) Characteristics of the fault-related rocks, fault zones and the principal slip zone in the Wenchuan Earthquake Fault Scientific Drilling Project Hole-1 (WFSD-1). Tectonophysics 584:23–42
Li Y, Zhou R, Zhao G, Li H, Su D, Ding H, Yan Z, Yan L, Yun K, Ma C (2014a) Tectonic uplift and landslides triggered by the Wenchuan earthquake and constraints on orogenic growth: a case study from Hongchun Gully, Longmen Mountains, Sichuan, China. Quat Int 349:142–152
Li G, West AJ, Densmore AL, Jin Z, Parker RN, Hilton RG (2014b) Seismic mountain building: landslides associated with the 2008 Wenchuan earthquake in the context of a generalized model for earthquake volume balance. Geochem Geophys Geosyst 15:833–844
Liu F, Fu BH, Yang SH (2013) Quantitative estimation of the evacuation time of landslide mass and sediment induced by the 2008 Wenchuan great earthquake along the Minjiang River, Longmen Shan in east Tibet. Chin J Geophys 56(5):1517–1525 (in Chinese with English abstract)
Liu-Zeng J, Zhang ZH, Wen L, Tapponnier P, Sun J, Xing XG, Hu G, Xu Q, Zeng LS, Ding L (2009) Co-seismic ruptures of the 12 May 2008, Ms 8.0 Wenchuan earthquake, Sichuan: east–west crustal shortening on oblique, parallel thrusts along the eastern edge of Tibet. Earth Planet Sci Lett 286:355–370
Liu-Zeng J, Wen L, Sun J, Zhang ZH, Hu GY, Xing XG, Zeng LS, Xu QA (2010) Surficial slip and rupture geometry on the Beichuan fault near Hongkou during the M(w) 7.9 Wenchuan Earthquake, China. Bull Seismol Soc Am 100:2615–2650
Liu-Zeng J, Wen L, Oskin M, Zeng LS (2011) Focused modern denudation of the Longmen Shan margin, eastern Tibetan Plateau. Geochem Geophys Geosyst 12:Q11007. doi:10.1029/2011gc003652
Malamud B, Turcotte D, Guzzetti F, Reichenbach P (2004) Landslides, earthquakes, and erosion. Earth Planet Sci Lett 229:45–59
Molnar P (2012) Isostasy can't be ignored. Nat Geosci 5:83
Molnar P, Anderson RS, Anderson SP (2007) Tectonics, fracturing of rock, and erosion. J Geophys Res 112:F03014. doi:10.1029/2005JF000433
Ouimet W (2010) Landslides associated with the May 12, 2008 Wenchuan earthquake: implications for the erosion and tectonic evolution of the Longmen Shan. Tectonophysics 491:244–252
Ouimet W (2011) The hills came tumbling down. Nat Geosci 4:424–425

Ouimet B, Whipple KX, Granger DE (2009) Beyond threshold hillslopes: channel adjustment to base-level fall in tectonically active mountain ranges. Geology 37:579–582

Parker RN, Densmore AL, Rosser NJ, de Michele M, Li Y, Huang RQ, Whadcoat S, Petley DN (2011) Mass wasting triggered by the 2008 Wenchuan earthquake is greater than orogenic growth. Nat Geosci 4:449–452

Qi SW, Xu Q, Lan HX, Zhang B, Liu JY (2010) Spatial distribution analysis of landslides triggered by 2008. 5.12 Wenchuan Earthquake, China. Eng Geol 116:95–108

Ran YK, Shi X, Wang H, Chen LC, Chen J, Liu RC, Gong HL (2010a) The maximum coseismic vertical surface displacement and surface deformation pattern accompanying the Ms 8.0 Wenchuan earthquake. Chin Sci Bull 55:841–850

Ran YK, Chen LC, Chen J, Wang H, Chen GH, Yin JH, Shi X, Li CX, Xu XW (2010b) Paleoseismic evidence and repeat time of large earthquakes at three sites along the Longmenshan fault zone. Tectonophysics 491:141–153

Ran YK, Chen WS, Xu XW, Chen LC, Wang H, Yang CC, Dong SP (2013) Paleoseismic events and recurrence interval along the Beichuan–Yingxiu fault of Longmenshan fault zone, Yingxiu, Sichuan, China. Tectonophysics 584:81–90

Ren Z, Zhang Z, Yin J, Dai F, Zhang H (2014a) Morphogenic uncertainties of the 2008 Wenchuan Earthquake: Generating or reducing? J Earth Sci 25:668–675

Ren Z, Zhang Z, Dai F, Yin J, Zhang H (2014b) Topographic changes due to the 2008 Mw 7.9 Wenchuan earthquake as revealed by the differential DEM method. Geomorphology 217:122–130

Rice R, Crobett E, Bailey R (1969) Soil slips related to vegetation, topography, and soil in southern California. Water Resour Res 5:647–659

Safran EB (2003) Geomorphic interpretation of low-temperature thermochronologic data: insights from two-dimensional thermal modeling. J Geophys Res Solid Earth 108(2189):2002J. doi:10.1029/B001870,2003

Simonett DS (1967) Landslide distribution and earthquakes in the Benwani and Torricelli Mountains, New Guinea a statistical analysis. Landform studies form Australia and New Guinea. Cambridge University Press, Cambridge, pp 64–84

Tian Y, Kohn BP, Gleadow AJ, Hu S (2013) Constructing the Longmen Shan eastern Tibetan Plateau margin: insights from low-temperature thermo-chronology. Tectonics 32:576–592

Wang EC, Meng QR (2009) Mesozoic and Cenozoic tectonic evolution of the Longmenshan fault belt. Sci China Ser D Earth Sci 52:579–592

Wang ZY, Shi WJ, Liu DD (2011) Continual erosion of bare rocks after the Wenchuan earthquake and control strategies. J Asian Earth Sci 40:915–925

Wen XZ, Zhang PZ, Du F, Long F (2009) The background of historical and modern seismic activities of the occurrence of the 2008 Ms 8.0 Wenchuan, Sichuan, earthquake. Chin J Geophys 52:444–454 (in Chinese with English abstract)

Xu XW, Wen XZ, Ye JQ, Ma BQ, Chen J, Zhou RJ, He HL, Tian QJ, He YL, Wang ZC, Zhao ZM, Feng XJ, Yu GH, Chen LC, Chen GH, Yu SE, Ran YK, Li XG, Li CX, An YF (2008) The Ms 8.0 Wenchuan earthquake surface ruptures and its seismogenic structure. Seismol Geol 30:597–629 (in Chinese with English abstract)

Xu XW, Wen XZ, Yu GH, Chen GH, Klinger Y, Hubbard J, Shaw J (2009a) Coseismic reverse-and oblique-slip surface faulting generated by the 2008 Mw 7.9 Wenchuan earthquake, China. Geology 37:515–518

Xu Q, Pei XJ, Huang RQ (2009b) Large-scale landlside induced by the Wenchuan earthquake. Science Press, Beijing (In Chinese)

Xu C, Xu X, Yao X, Dai F (2014) Three (nearly) complete inventories of landslides triggered by the May 12, 2008 Wenchuan Mw 7.9 earthquake of China and their spatial distribution statistical analysis. Landslides 11:441–461

Yang XJ, Chen LD (2010) Using multi-temporal remote sensor imagery to detect earthquake-triggered landslides. Int J Appl Earth Obs Geoinf 12:487–495

Yin YP, Cheng YL, Wan J, Wang M, Liu B, Song Y, Liang JT (2011) Remote sensing research on Daguangbao gigantic rockslide triggered by Wenchuan earthquake. J Eng Geol 19:674–684

Zhang PZ, Xu XW, Wen XZ, Ran YK (2008) Slip rates and recurrence intervals of the Longmen Shan active fault zone, and tectonic implications for the mechanism of the May 12 Wenchuan earthquake, 2008, Sichuan, China. Chin J Geophys 51:1066–1073 (in Chinese with English abstract)

Zhang ZJ, Wang YH, Chen Y, Houseman GA, Tian XB, Wang EC, Teng JW (2009) Crustal structure across Longmenshan fault belt from passive source seismic profiling. Geophys Res Lett. doi:10.1029/2009GL09580

Zhang PZ, Wen XZ, Shen ZK, Chen J (2010a) Oblique, high-angle, listric-reverse faulting and associated development of strain: the Wenchuan earthquake of May 12, 2008, Sichuan, China. Annu Rev Earth Planet Sci 38:353–382

Zhang ZJ, Yuan XH, Chen Y, Tian XB, Kind R, Li XQ, Teng JW (2010b) Seismic signature of the collision between the east Tibetan escape flow and the Sichuan Basin. Earth Planet Sci Lett 292:254–264